The International Maritime Transport and Logistics (MARLOG 14) - ISSN 2974-3141
http://dx.doi.org/10.21622/MARLOG.2025.14.1.43
Artificial Intelligence Implementations Towards Shaping the Future of Digital World

A STUDY OF PASSIVE FLOW ON NATO-GD SHIP MODEL AIRWAKE USING COMPUTATIONAL FLUID DYNAMICS

Abd Elmenaim H. Alaktaa [1], Salaheldin A. Mohamad [2], Ahmed S. Shehata [1] And Khaled Elsherbiny [1]

(1) Marine and Offshore Engineering Department, College of Engineering and Technology, Arab Academy for Science Technology and Maritime Transport, Alexandria, Egypt, khaled.elsherbiny@aast.edu.

(2) Ships & Submarines Department, Military Technical College, Kobry Elkobbah, Cairo, Egypt .

ABSTRACT

This study focuses on numerically analysing the passive flow control method for manipulating air wakes on the NATO-GD ship model using detached eddy simulation (DES). The numerical techniques are verified through comparison with experimental data obtained from the NATO-GD baseline. To develop the flow control model, the hanger base of the original NATO-GD ship model is altered by incorporating a curved roof edge. The findings indicate distinct performances in vortex structure on the flight deck between the two cases, along with variations in turbulent characteristics. Specifically, the results demonstrate that the curved roof edge directs flow more effectively towards the low-speed area (LSA) on the deck, leading to improved reduction of flow recirculation and enhanced recovery of streamwise velocity. How-ever, this modification also results in higher levels of turbulent kinetic energy (TKE) in the air wake.

Keywords: Air wake, Frigate flow control, passive, NATO-GD model, Flight deck, CFD.

1. INTRODUCTION

The operation of launching and recovering helicopters on naval vessels poses considerable dif-ficulties for pilots. The limited size of the landing decks is susceptible to movement resulting from the ship's pitch, roll, and substantial motions. As the vessel advances and interacts with the wind, the airflow over the superstructure generates a disturbed flow region referred to as the ship airwake above the flight deck. This airwake is characterized by turbulent structures that fluctuate over time due to flow separation around the ship's architecture and the intricate interplay of unstable shear layers and vortices. These elements can significantly influence the handling characteristics of the aircraft. To improve the safety of helicopter operations aboard ships, flow control strategies may be employed to alleviate the negative impacts of the airwake by modifying the design of the ship's superstructure.

Many studies have been carried out to investigate both active and passive flow control. In par-ticular, The adverse impact of the unsteady ship air wake on helicopter operations has been effectively addressed by (Kääriä et al. 2013) through an experimental study involving aerodynamic modifications to a model scale generic ship (SRF) shortened research frigate. By altering the superstructure, the authors were able to mitigate this issue and accurately measure the resulting force and moment. The findings revealed that all the ship modifications significantly reduced the root mean square (RMS) force and moments when compared to the baseline ship geometry. In a wind tunnel, (Bardera and Meseguer 2015) conducted an experimental study involving a model of a simple frigate shape (SFS). The study aimed to test four different roof configurations, all of which involved rounding the sharp edges of the hanger model. This modification aimed to minimize the impact of the wake flow above the flight deck and reduce the risks associated with onboard helicopter operations. The study's

results revealed a significant effect when utilizing the rounded the sharp edges of the hanger model, which showed the highest cur-vature degree. This configuration led to a remarkable reduction in the shear layer more than 42%. In their (Gallas et al. 2017) study, they conducted an experiment in a wind tunnel to address the complex flow patterns encountered during helicopter launch and recovery operations. They aimed to improve these flow patterns by implementing active flow control through continuous steady blowing from slots located at the periphery of the hanger. The ejected mass flow was directed tangentially to the free stream using a simple frigate onera (SFO). To measure the velocity and turbulent characteristics of the fluid flow, the authors employed the hot wire anatomy technique. The results of the study revealed a reduction in the recirculation region within the air wake flow above the helicopter deck. An experimental investi-gation was conducted by (Carlos Matías-García, Nicolás Franchini-Longhi, and Bardera 2019) to ex-amine the effects of active flow control (AFC) techniques. The study utilized wind tunnel tests and Particle Image Velocimetry (PIV) to obtain velocity maps. The authors focused on reducing the size of recirculation bubbles and balancing incident velocities on the helicopter rotor by applying suction over various surfaces of the hanger, including the door, roof, and sidewalls. In comparison to previous studies that employed passive flow control techniques using trapezoidal vortex generators to generate vortices downstream without requiring additional energy on small naval vessels, the authors observed a decrease in the area of the low velocity region more than 14%. (SHI et al. 2019) conducted additional CFD sim-ulations to study the effects of three aerodynamic modifications (ramp, notch, and flap) on a 1/2-scale landing platform dock-17 (LPD-17) ship under different WOD conditions. The focus was on analyzing the impact of these modifications on rotor air loads using the RADAS solver. The results showed that the ramp and notch modifications reduced turbulence intensity and oscillatory rotor air loading, while the flap modification had negative effects on the flow field. The modifications improved shedding vor-tices, flow separation, and normal force on the rotor. However, ship air wake caused significant oscilla-tions in rotor forces during landing. The authors concluded that Flow control devices like ramps and notches can enhance safety by reducing turbulence and rotor air loading, but their design should be carefully considered to avoid introducing additional vortices and disturbances.

2. Model description

The existing body of research on ship air-wake predominantly centers on the Simplified Frigate Ship model 2 (SFS2). This model represents an advancement over its predecessor, the Simplified Frigate Ship (SFS), which was created by The Technical Corporation Program (TTCP) (Wilkinson et al. 1998). The primary objective of developing the SFS was to create a simplified baseline model that could serve as a foundation for collaborative research on the ship-helicopter dynamic interface. By offering an open domain model, it sought to promote international cooperation in this area. The design of the SFS model was limited by the available computational and fabrication resources, leading to its construction from a series of cuboid structures. The model comprised only three topside elements: the superstructure, land-ing deck, and funnel. The configuration of the flight deck in the SFS bore a rough resemblance to that of the ANZAC and FFG-7 frigates utilized by the Royal Australian Navy (Toffoletto, Reddy, and Lewis 2003). In 2001, an additional bow was added to the original design, resulting in the SFS2. Since its introduction, the SFS2 has been widely employed to improve computational fluid dynamics (CFD) mod-eling (Syms 2008); (Yuan, Wall, and Lee 2018a); (Rui et al. 2015) and to investigate novel experimental techniques ((Taymourtash et al. 2021); (Sydney, Ramsey, and Milluzzo 2017); (Toffoletto, Reddy, and Lewis 2003). The application of the SFS2 model in research is further supported by studies (Orbay and Sezer-Uzol 2016); (Shrish Shukla et al. 2020); (Shi et al. 2017), which include simulations both with and without rotor downwash. This facilitates the development of integrated simulations that link turbu-lent air-wake dynamics with helicopter flight models (Sharma et al. 2019); (Bludau et al. 2017). Insights gained from SFS2 research on air-wake are primarily utilized in flight simulations to depict the variable flow fields that pilots may experience during helicopter landings on ship decks (Hodge et al. 2009). The SFS2 model continues to be a prevalent choice among researchers, despite the emergence of more com-plex and realistic ship models. Recent studies, such as those by (Bardera, Matías, and Barroso 2021), (Farish et al. 2020), and (S. Shukla et al. 2021), have utilized this simplified model to explore ship air-wake phenomena,

suggesting its ongoing relevance in future research in this area. However, various investigations, including those by (Rahimpour and Oshkai 2019), (Yuan, Wall, and Lee 2018a), (Taymourtash et al. 2021), and (Dooley et al. 2020), have indicated that the flow dynamics over heli-copter platforms on ships are significantly affected by the geometrical configurations of the vessels. Furthermore, (Owen et al. 2021a) have argued that the slender profile of the SFS2 model no longer accurately reflects the design of many contemporary ships, particularly frigates and destroyers. (Lavers 2012) has pointed out that modern combat vessels are engineered with stealth features to minimize radar visibility. For instance, in contrast to the SFS2, the sides of these modern ships are characterized by a flat, vertical surface that slopes sharply inward. Considering these advancements, the NATO-Applied Vehicle Technology group has recently introduced the North Atlantic Treaty Organization-Generic De-stroyer (NATO-GD) model (Owen et al. 2021a). This model, unlike the SFS2, showcases a more detailed geometry, complete with an elaborate superstructure, integrated mast, exhaust stack, and radar, designed to resemble contemporary naval combatants without being tied to any specific class.

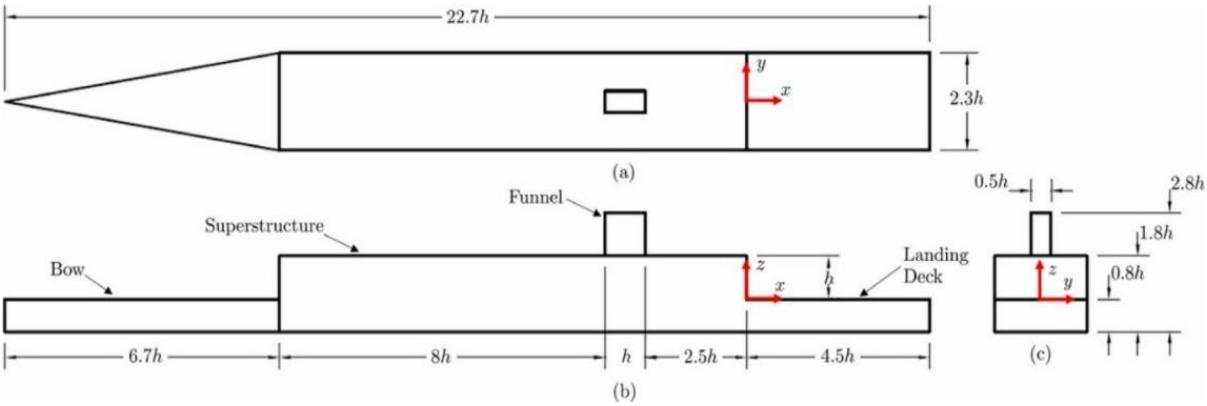

Figure 1: Schematic illustration of the SFS2 model: (a) top view, (b) side view, (c) rear view. The hangar's full-scale dimension (ℎ) is 6 meters.

This Study Focuses on The Application of The Passive Flow Control Technique on the NATO-GD ship model, which shares similarities in design with modern naval combat ships and possesses a complex superstructure (Setiawan et al. 2022). The effectiveness of this technique is validated using the numerical method known as detached eddy simulation (DES), which is compared against experimental data obtained from the baseline NATO-GD ship model without flow control. The passive flow control technique is then implemented along one edge of both the baseline NATO-GD and the modified NATO-GD, which features a curved roof edge. The objective of this research is to investigate the impact of these modifications on air wake manipulations, specifically in terms of the low-speed area (velocity profile) and Turbulent kinetic energy (TKE). By achieving a more precisely designed control effective-ness of the ship's air wake, this paper aims to enhance our understanding of the control mechanism within this new context.

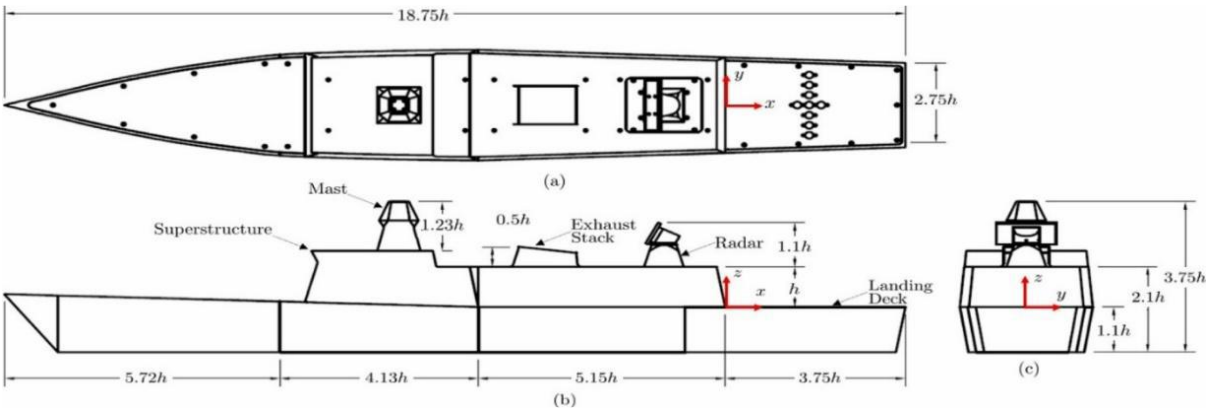

Figure 2: Schematic illustration of the NATO - GD ship model: (a) top view, (b) side view, (c) rear view. The hangar's full - scale dimension (⁄) is 8 meters. The scale of the model is 1:50.

3. NUMERICAL METHOD

Detached Eddy simulation (DES) has been employed in previous studies by (Forrest et al. 2012), as well as more recently by (Yuan, Wall, and Lee 2018b) and (Gao and Liu 2016). The DES is conducted using the finite volume software, star-CCM+. The governing equations utilized in this simulation are the incompressible, spatially filtered 3D Navier-Stokes equations. These equations capture the unstead-iness associated with the large-scale turbulent motion and model the small-scale high-frequency com-ponents of the fluid motion. (Forrest and Owen 2010) adopted a non-dimensional time step of $\nabla t*$= 1.88×10−2 (1).

By substituting this value into a recommended time step size of ∇t = 0.02 s is obtained for a NATO-GD air wake simulation. This ensures that the CFL (Courant-Friedrichs-Lewy) number remains lower than 1 in over 99% of the cells.

$$\nabla t* = \nabla t\, Vrw/B \qquad (1)$$

were,

$\nabla t*$ is the non-dimensional timestep size.

B is the ship beam (at the flight deck B = 19 m)

∇t is simulation timestep size.

Vrw is the reference or free stream wind speed (Vref = 20m/s).

The Computational Domain, as stated in the NATO Task Group AVT-217 report (Owen et al. 2021a), requires specific boundary conditions. The upstream boundary should be positioned at a distance of at least two ship lengths (Ls) ahead of the ship, while the downstream boundary should be located at least 3Ls behind the ship. Additionally, the sides of the domain should be at a minimum distance of Ls from the ship Figure 3. Furthermore, the height of the domain should extend at least 300m above the water plane. In contrast, (Yuan, Wall, and Lee 2018b) defines the domain boundaries differently. It uti-lizes inlet and outlet boundaries, with the top and side boundaries treated as free-slip walls Figure 4. To ensure grid independence, a study was conducted using three different mesh configurations. These in-clude an initial mesh with a certain number of cells, a coarse mesh with a different number of cells, and a fine mesh with yet another number of cells.

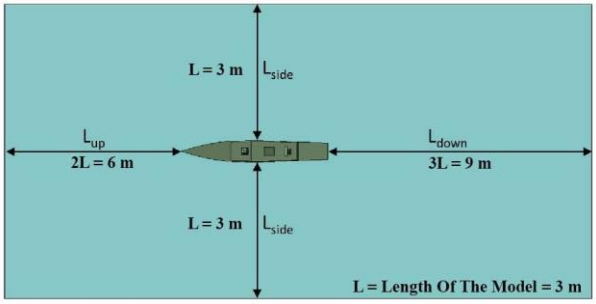

Figure 4: Computational Domain dimensions. - GD baseline.

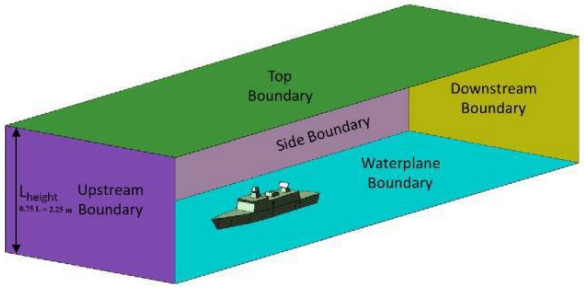

Figure 4: Boundary Condition of NATO

3.1. Mesh Sensitivity

In order to assess grid independence, three different grid spacings (∇0) were examined based on the guidelines (Spalart and Streett 2001). The baseline ∇0 was selected and then adjusted both upwards and downwards by a factor of √2. The computations were conducted for a headwind at a

freestream speed of 20 m/s, with the grids identified as Mesh1 (10,830,916 cells), Mesh2 (13,944,522 cells), and Mesh3 (17,251,699 cells). When comparing the reattachment length over the helicopter deck for the three grids, minimal differences were observed in the results, The reattachment length refers to the dis-tance downstream from the helicopter hangar on a helicopter deck where the separated airflow due to the hangar's obstruction reattaches to the deck Figure 5. Figure 6 displays the reattachment length acting on helicopter deck. It is evident that none of the grids exhibit a significant enhancement compared to the experimental data (Owen et al. 2021b). The similarity in the results from the three sets, despite variations in cell size, suggests grid-independent solutions. Although the coarser Mesh1 grid seems to yield satisfactory results in terms of average quantities, it is important to emphasize that the objective of these computations is to provide precise unsteady data for simulation purposes. A coarser grid neces-sitates a larger time step to maintain an appropriate Courant number; for Mesh3, this would correspond to a high computational effort. Given that the output from these computations will be utilized to generate unsteady air-wake data for piloted flight simulations, it was deemed necessary to have a higher air wake update frequency to ensure a sufficient level of simulator accuracy. The computational time and memory requirements for Mesh2 were manageable within the computer cluster's capabilities, leading to the de-cision to utilize Mesh2 for all subsequent computations to guarantee satisfactory spatial and temporal resolutions.

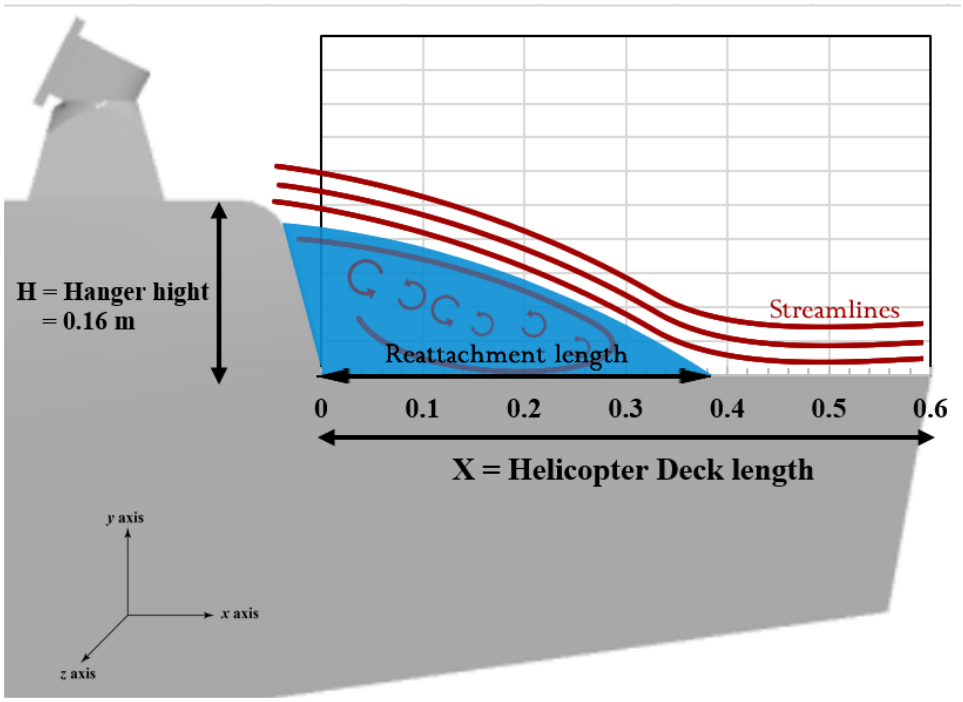

Figure 5: Graphical scheme for Reattachment length definition along NATO - GD model helicopter deck .

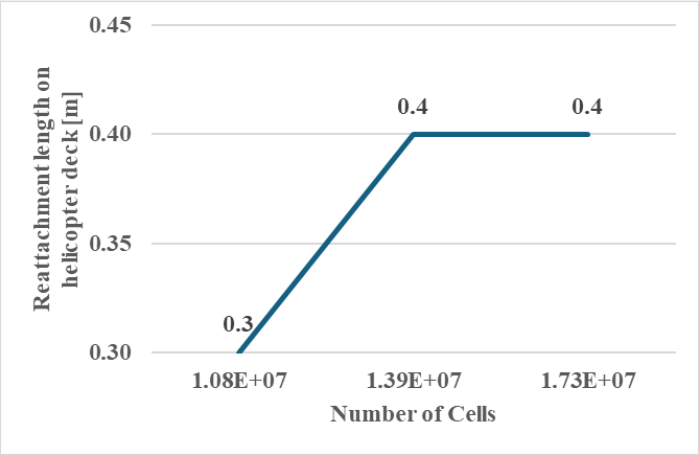

Figure: 6 Mesh Sensitivity for NATO-GD Model

	Number of cells	Reattachment length [m]
Mesh 1	1.08E+07	0.35
Mesh 2	1.39E+07	0.39
Mesh 3	1.73E+07	0.39

Table 1: Results of Mesh Sensitivity Study

3.2. NATO-GD Model Validation

The validation of the numerical method involves a comparison between the pressure obtained from the numerical simulation and the pressure measured experimentally. The pressure measurement is conducted at the center of the deck, as depicted in Figure 7.

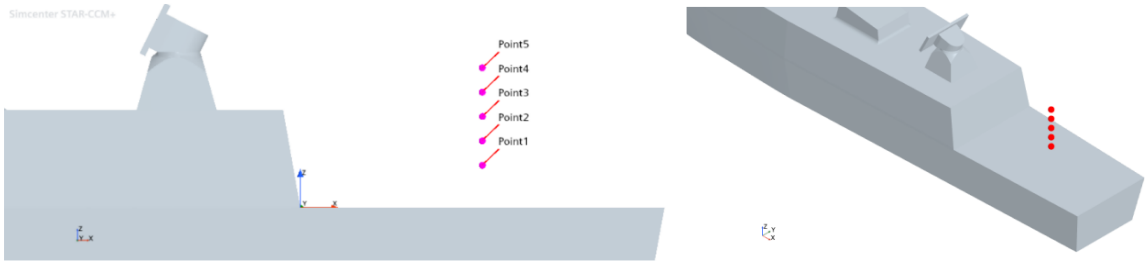

Figure 7: Points At Pressure Prboes At Center Line Above The Helicopter Deck

	Point 1	Point 2	Point 3	Point 4	Point 5
x	0.3000	0.3000	0.3000	0.3000	**0.3000**
y	0.0000	0.0000	0.0000	0.0000	**0.0000**
z	0.0700	0.1100	0.1500	0.1900	**0.2300**
Pressure (Experimental) [PSI]	14.6000	14.5845	14.5866	14.5867	**14.4666**
Pressure (Numerical) [PSI]	14.6947	14.6942	14.6949	14.6950	**14.6944**
ΔP	0.0947	0.1097	0.1083	0.1083	**0.2278**
Error	0.65%	0.75%	0.74%	0.74%	**1.57%**

Table 2 The Placement of Pressure Probes with The Experimental and Numerical Measured Pressure

By comparing the predicted pressure values with the measured ones Table 2, the deviations from the experimental results, denoted as ΔP, are determined. At point 5, which represents the maximum deviation, the pressure is found to deviate from the experiment by 1.57%. On the other hand, at point 1, which represents the minimum deviation, the pressure is found to deviate from the experiment by 0.65%. Subsequently, the pressure distribution along the center of the deck is utilized for further validation purposes. Figure 9 illustrates the satisfactory agreement between the predicted and measured pressure distributions. This indicates that the current numerical method is capable of accurately predicting the flow around the NATO-GD model. Furthermore, the grid independence is successfully achieved with a mesh size of 13944522 cells.

4. NUMERICAL RESULTS OF THE BASELINE AND FLOW CONTROL CASE.

The outcomes of the controlled ship flow are outlined in this section. Two scenarios are exam-ined for comparison: the NATO-GD base line and the NATO-GD modified model featuring a rounded-back hanger with r=100 mm. The findings by (Bardera and Meseguer 2015) demonstrate that the maxi-mum radius yields the highest impact. Nevertheless, it does not influence the volume of the hanger. (see Figure 8).

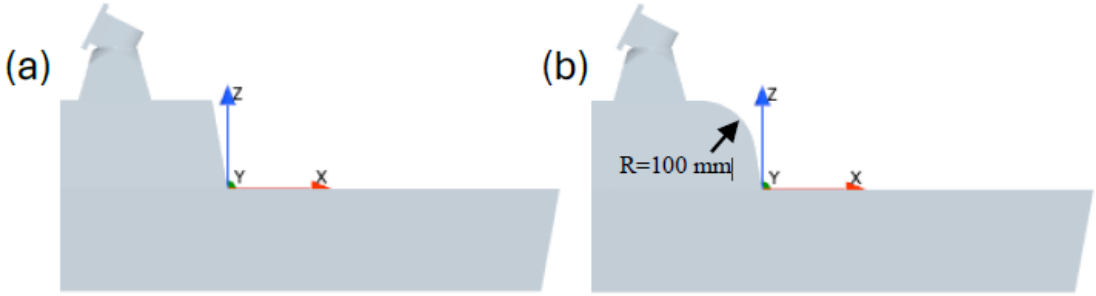

Figure 8 (a) NATO-GD Model, (b) NATO-GD Modiefied Model

The main feature of the flow is a large area where the air moves in circles below the unsteady and separated shear layer. This shear layer works like a mixing layer, where organized patterns form and move downstream. However, the lifespan of these structures is relatively short as they disintegrate before reattaching to the surface. Due to the turbulent nature of this phenomenon, reattachment is not constant and requires definition by a region rather than a single point. This variation is one of the con-tributing factors that adds complexity to helicopter landings,

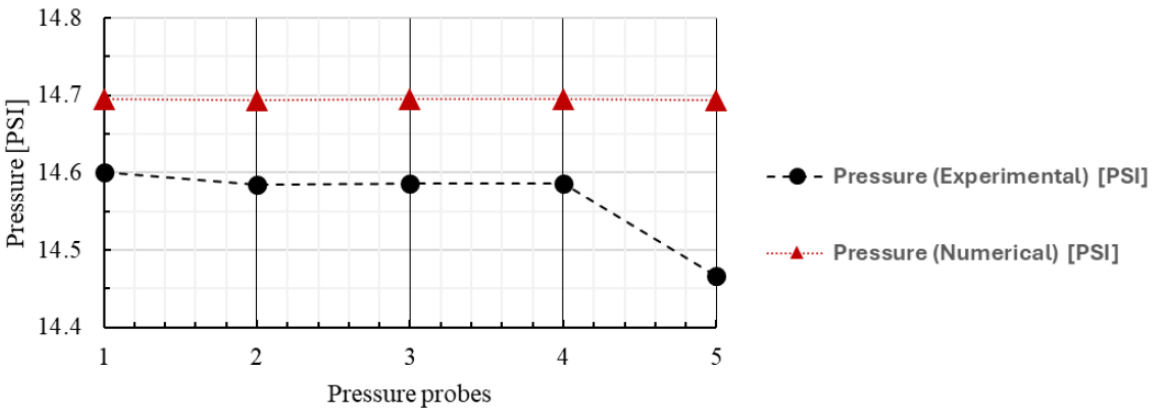

Figure 9 The Pressure Distribution At The Center Of Helicopter Deck.

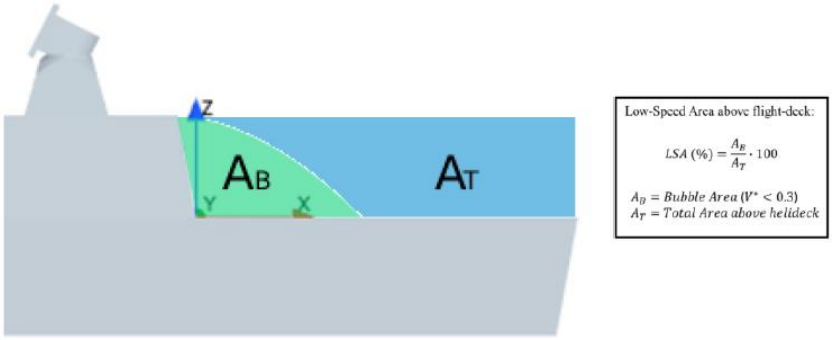

Figure 10 Graphical representation for comparative analysis: delineation of bubble and overall helideck areas, Low- Speed Area proportion over the flight-deck (LSA)

especially when the landing area is near this reattachment region, A crucial variable among the mean quantities is the velocity of the flow in the direction of the ship deck. A greater incoming flow velocity facilitates the takeoff of a helicopter with an increased overall weight (Shafer and Ghee 2005). Figure 11 shows the time-averaged U/Uref contours at three sections along x-z plane at y= 0, y= 0.12 m and y= -0.12 m to compare the two models (a) NATO-GD Base Model and (b) NATO-GD Modified Model. At all three sections, a region with low speed is evident in two instances. The negative velocity inside the recirculation region is depicted by the white region, and notably, case (b) featuring a rounded-back hanger shows a substantial reduction in size.

To facilitate the quantification of the various cases examined, a comprehensive comparison was conducted. This analysis concentrated on the dimensions of the low-velocity zone situated above the frigate's flight deck, as well as the velocity profile encountered by a helicopter rotor during the landing approach. To assess the area encompassed by the low-velocity region, a parameter termed Low-Speed Area above the flight deck (LSA) has been established, as illustrated in Figure 10. Regarding velocity, the bubble area (AB) is defined as the flow region characterized by a non-dimensional velocity (V∗) that falls below zero.

For the base configuration, the size of the recirculation bubble results in an LSA of 26.2%. However, when a rounded-back hanger with a radius of 100mm is implemented, the LSA is reduced by 3.9% to 22.5%.

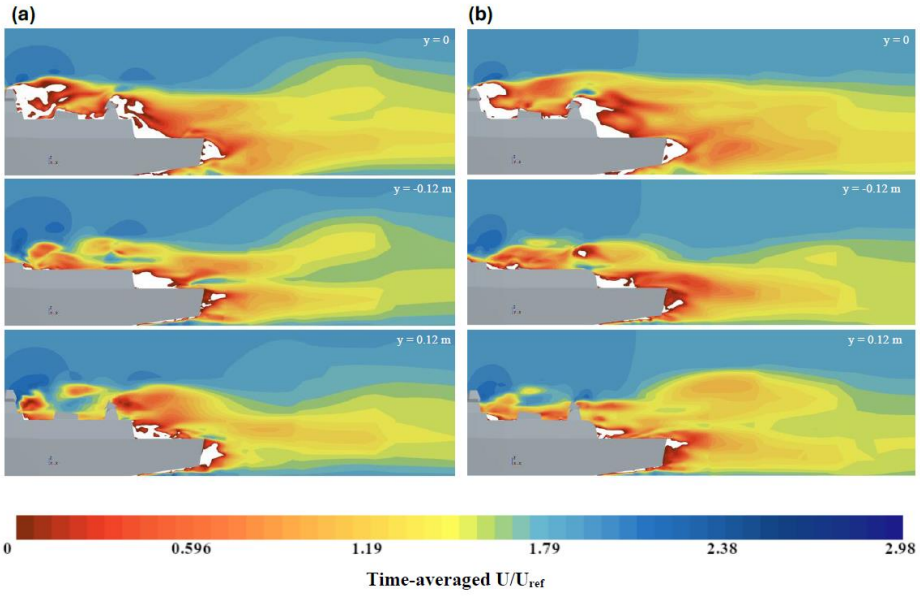

Figure 11: time-averaged U/Uref dimensionless velocity contours at three sections for (a) NATO-GD baseline (b) NATO-GD Modified Model

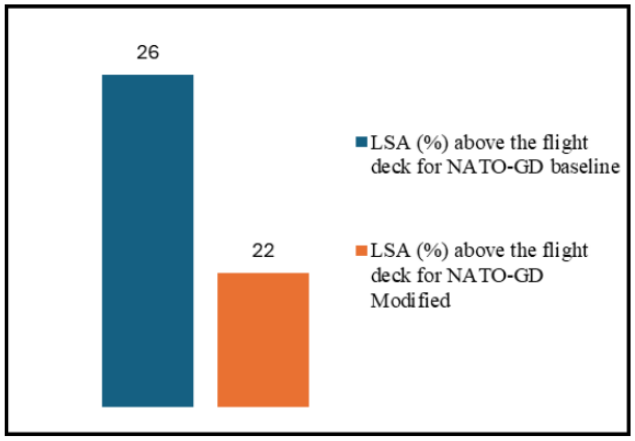

Figure 12 Low-Speed Area (LSA) above flight deck of the (a) NATO-GD baseline (b)NATO-GD modified Model.

The turbulent fluctuation is a significant element that contributes to the increased workload of pilots during the recovery (landing) of a maritime helicopter. The specific area affected by turbulent fluctuation varies depending on the chosen recovery procedure (Owen et al. 2021a). Figure 13 illustrates the locations where the helicopter recovery procedure takes place.

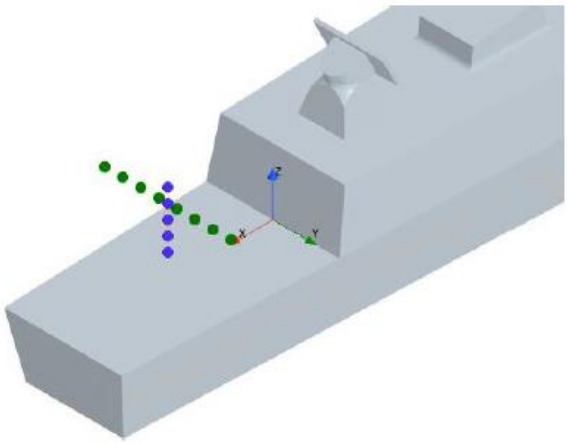

Figure 13: horizontal points at the helicopter recovery procedure and vertical Hovering points

To demonstrate the influence of the current Passive flow control on the turbulent fluctuations at the concerned region, the turbulent kinetic energy (TKE) is used here for discussion (2).

$$TKE = 0.5\left(\overline{\acute{u}\acute{u}} + \overline{\acute{v}\acute{v}} + \overline{\acute{\omega}\acute{\omega}}\right) \qquad (2)$$

TKE is normalized by the square of the Reference velocity U_{REF}.

The TKE is significantly elevated in case (b), for a more explicit presentation Figure 15. The data for case (b) exhibit values that are greater around the central line point compared to case (a) Figure 14 Figure 16. This implies that the shear stress indicates the existence of a velocity gradient along the y-direction, with higher shear stress corresponding to larger velocity gradients (in magnitude). These find-ings are consistent with the observations presented in Figure 15, where regions of high shear stress can be identified at the boundary between high and low-speed regions (Xu et al. 2023). Figure 14 illustrates the TKE values at the hovering points depicted in Figure 13. It is evident that the TKE values at the upper two points in case (b) are greater than those in case (a), indicating a less favorable outcome.

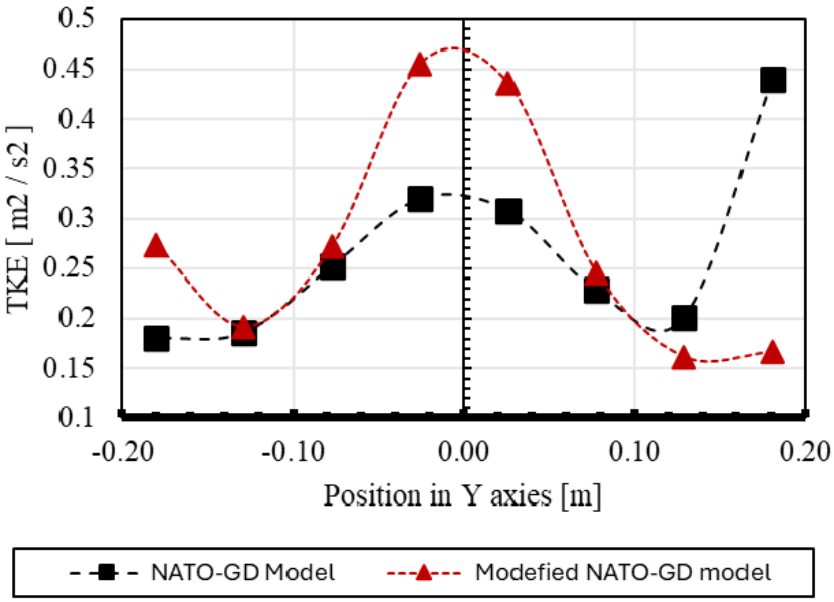

Figure 14: Plot of the time - averaged TKE along y direction

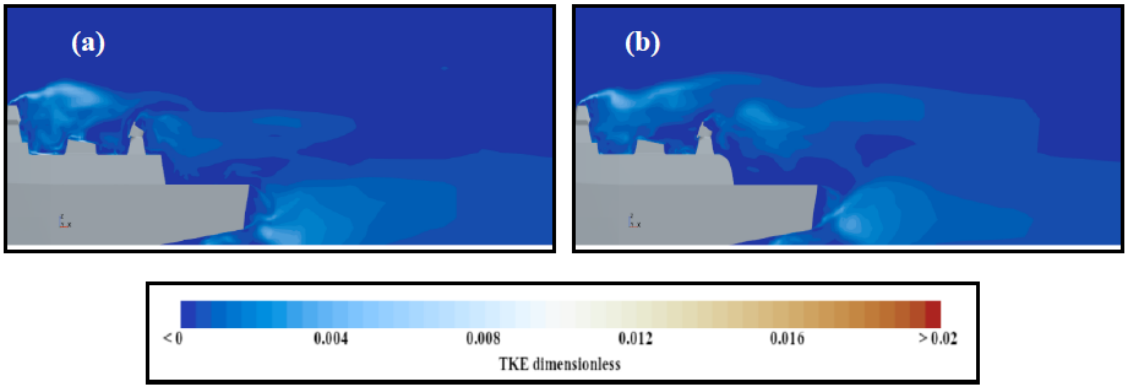

Figure 15 Turbulent Kinetic Energy (TKE) contour on the ship centerline for the simulated cases (a) Base NATO-GD model (b) NATO-GD Modified model

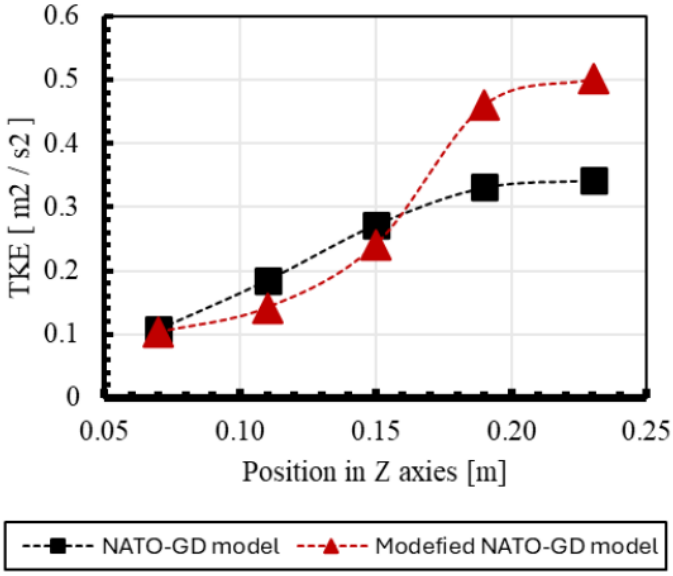

Figure 16: Plot of the time - averaged TKE along z direction at the hovering line.

5. CONCLUSION

The current study examines the passive flow control technique applied to the NATO-GD ship model for the purpose of controlling the airflow around the ship. The effectiveness of this control tech-nique is investigated through numerical analysis using detached eddy simulation (DES), which is then validated using experimental data obtained from the baseline NATO-GD ship model. To create the flow model, modifications are made to the hanger base of the baseline model by incorporating a curved roof edge. The results indicate that the two cases exhibit variations in vortex structure on the flight deck and turbulent quantities in the air wake. It is observed that the curved roof edge directs the flow more towards the low-speed area (LSA) on the deck, thereby effectively suppressing the LSA. This is advantageous for helicopter landing and takeoff as it leads to higher streamwise velocity and lower turbulent kinetic energy (TKE). However, it should be noted that the curved roof edge reduces the LSA while increasing the TKE in the air wake near the center region, owing to the enhanced shear stress in that region.

6. REFERENCES

7. Bardera, R., and J. Meseguer. 2015. "Flow in the near Air Wake of a Modified Frigate." Proceedings of the Institution of Mechanical Engineers, Part G: Journal of Aerospace Engineering 229 (6): 1003–12. https://doi.org/10.1177/0954410014542449.
8. Bardera, R, J C Matías, and E Barroso. 2021. "Experimental and Numerical Simulations of Simple Frigate with Suction Flow Control over the Deck." Ocean Engineering 236:109464. https://doi.org/https://doi.org/10.1016/j.oceaneng.2021.109464.
9. Bludau, Jakob, Juergen Rauleder, Ludwig Friedmann, and Manfred Hajek. 2017. "Real-Time Simulation of Dynamic Inflow Using Rotorcraft Flight Dynamics Coupled with a Lattice-Boltzmann Based Fluid Simulation." In 55th AIAA Aerospace Sciences Meeting, 50.
10. Carlos Matías-García, Juan, Sebastian Nicolás Franchini-Longhi, and Rafael Bardera. 2019. "Vortex Generators and Active Flow Control in the Aft-Deck of a Frigate." https://doi.org/10.13009/EUCASS2019-322.
11. Dooley, Gregory, J Ezequiel Martin, James H J Buchholz, and Pablo M Carrica. 2020. "Ship Airwakes in Waves and Motions and Effects on Helicopter Operation." Computers & Fluids 208:104627. https://doi.org/https://doi.org/10.1016/j.compfluid.2020.104627.

12. Farish, David, Dhuree Seth, Regis Thedin, and Sven Schmitz. 2020. "Investigations of Ship Airwakes Using Concurrent Computations and Experiments." In Vertical Flight Society's 76th Annual Forum and Technology Display.
13. Forrest, James S, and Ieuan Owen. 2010. "An Investigation of Ship Airwakes Using Detached-Eddy Simulation." Computers & Fluids 39 (4): 656–73. https://doi.org/https://doi.org/10.1016/j.compfluid.2009.11.002.
14. Forrest, James S, Ieuan Owen, Gareth D Padfield, and Steven J Hodge. 2012. "Ship-Helicopter Operating Limits Prediction Using Piloted Flight Simulation and Time-Accurate Airwakes." Journal of Aircraft 49 (4): 1020–31. https://doi.org/10.2514/1.C031525.
15. Gallas, Q., M. Lamoureux, J. C. Monnier, A. Gilliot, C. Verbeke, and J. Delva. 2017. "Experimental Flow Control on a Simplified Ship Helideck." AIAA Journal 55 (10): 3356–70. https://doi.org/10.2514/1.J055902.
16. Gao, Zhe-Ming, and Chang-Meng Liu. 2016. "Airwake Characteristics Simulations with Different Turbulence Models BT - Proceedings of the 2016 5th International Conference on Advanced Materials and Computer Science." In , 329–32. Atlantis Press. https://doi.org/10.2991/icamcs-16.2016.70.
17. Hodge, Steven J, Steven J Zan, David M Roper, Gareth D Padfield, and Ieuan Owen. 2009. "Time-accurate Ship Airwake and Unsteady Aerodynamic Loads Modeling for Maritime Helicopter Simulation." Journal of the American Helicopter Society 54 (2): 22005.
18. Kääriä, Christopher H., Yaxing Wang, Mark D. White, and Ieuan Owen. 2013. "An Experimental Technique for Evaluating the Aerodynamic Impact of Ship Superstructures on Helicopter Operations." Ocean Engineering 61:97–108. https://doi.org/10.1016/j.oceaneng.2012.12.052.
19. Lavers, Christopher. 2012. Reeds Vol 14: Stealth Warship Technology. A&C Black.
20. Orbay, Ezgi, and Nilay Sezer-Uzol. 2016. "Computational Fluid Dynamics Simulations of Ship Airwake with a Hovering Helicopter Rotor." In Ninth International Conference on Computational Fluid Dynamics. Istanbul.
21. Owen, Ieuan, Richard Lee, Alanna Wall, and Nicholas Fernandez. 2021a. "The NATO Generic Destroyer – a Shared Geometry for Collaborative Research into Modelling and Simulation of Shipboard Helicopter Launch and Recovery." Ocean Engineering 228:108428. https://doi.org/https://doi.org/10.1016/j.oceaneng.2020.108428.
22. ———. 2021b. "The NATO Generic Destroyer – a Shared Geometry for Collaborative Research into Modelling and Simulation of Shipboard Helicopter Launch and Recovery." Ocean Engineering 228 (May). https://doi.org/10.1016/j.oceaneng.2020.108428.
23. Rahimpour, Mostafa, and Peter Oshkai. 2019. "The Effects of Unsteady Change in Wind Direction on the Airflow over the Helicopter Platform of a Polar Icebreaker." Ocean Engineering 172:22–30. https://doi.org/https://doi.org/10.1016/j.oceaneng.2018.11.049.
24. Rui, Zhao, Rong Ji-Li, Li Hai-Xu, and Zhao Peng-Cheng. 2015. "Entropy-Based Detached-Eddy Simulation of the Airwake over a Simple Frigate Shape." Advances in Mechanical Engineering 7 (11): 1687814015616930.
25. Setiawan, Heri, Kevin, Jimmy Philip, and Jason P Monty. 2022. "Turbulence Characteristics of the Ship Air-Wake with Two Different Topside Arrangements and Inflow Conditions." Ocean Engineering 260:111931. https://doi.org/https://doi.org/10.1016/j.oceaneng.2022.111931.
26. Shafer, Daniel, and Terence Ghee. 2005. "Active and Passive Flow Control over the Flight Deck of Small Naval Vessels." In 35th AIAA Fluid Dynamics Conference and Exhibit. Fluid Dynamics and Co-Located Conferences. American Institute of Aeronautics and Astronautics. https://doi.org/doi:10.2514/6.2005-5265.
27. Sharma, Abhinav, Jiayang Xu, Ashwani K Padthe, Peretz P Friedmann, and Karthik Duraisamy. 2019. "Simulation of Maritime Helicopter Dynamics during Approach to Landing with Time-Accurate Wind-over-Deck." In AIAA SciTech 2019 Forum, 861.
28. SHI, Yongjie, Xiang HE, Yi XU, and Guohua XU. 2019. "Numerical Study on Flow Control of Ship Airwake and Rotor Airload during Helicopter Shipboard Landing." Chinese Journal of Aeronautics 32 (2): 324–36. https://doi.org/10.1016/j.cja.2018.12.020.

29. Shi, Yongjie, Yi Xu, Kun Zong, and Guohua Xu. 2017. "An Investigation of Coupling Ship/Rotor Flowfield Using Steady and Unsteady Rotor Methods." Engineering Applications of Computational Fluid Mechanics 11 (1): 417–34. https://doi.org/10.1080/19942060.2017.1308272.
30. Shukla, S., S. N. Singh, S. S. Sinha, and R. Vijayakumar. 2021. "Comparative Assessment of URANS, SAS and DES Turbulence Modeling in the Predictions of Massively Separated Ship Airwake Characteristics." Ocean Engineering 229. https://doi.org/10.1016/j.oceaneng.2021.108954.
31. Shukla, Shrish, Sidh N Singh, Sawan S Sinha, and R Vijayakumar. 2020. "A Conceptual Method to Assess Ship-Helicopter Dynamic Interface." Proceedings of the Institution of Mechanical Engineers, Part G: Journal of Aerospace Engineering 234 (5): 1092–1116. https://doi.org/10.1177/0954410019896741.
32. Spalart, Philippe, and Craig Streett. 2001. "Young-Person's Guide to Detached-Eddy Simulation Grids," August.
33. Sydney, Anish J, Joseph Ramsey, and Joseph Milluzzo. 2017. "Time-Resolved Piv Measurements of Ship Motion and Orientation Effects on Airwake Development." In 35th AIAA Applied Aerodynamics Conference, 4230.
34. Syms, G. F. 2008. "Simulation of Simplified-Frigate Airwakes Using a Lattice-Boltzmann Method." Journal of Wind Engineering and Industrial Aerodynamics 96 (6–7): 1197–1206. https://doi.org/10.1016/j.jweia.2007.06.040.
35. Taymourtash, Neda, Daniele Zagaglia, Alex Zanotti, Vincenzo Muscarello, Giuseppe Gibertini, and Giuseppe Quaranta. 2021. "Experimental Study of a Helicopter Model in Shipboard Operations." Aerospace Science and Technology 115:106774. https://doi.org/https://doi.org/10.1016/j.ast.2021.106774.
36. Toffoletto, R, K R Reddy, and J Lewis. 2003. "Effect of Ship Frontal Variation on the Flow Field in the Flight-Deck Region BT - Computational Fluid Dynamics 2002." In , edited by Steve W Armfield, Patrick Morgan, and Karkenahalli Srinivas, 191–96. Berlin, Heidelberg: Springer Berlin Heidelberg.
37. Wilkinson, C H, S J Zan, N E Gilbert, and J D Funk. 1998. "Modelling and Simulation of Ship Air Wakes for Helicopter Operations-a Collaborative Venture." In RTO AVT Symposium.
38. Xu, Kewei, Xinchao Su, Yutao Xia, Yitong Wu, Rickard Bensow, and Sinisa Krajnovic. 2023. "Active Flow Control of the Airflow of a Ship at Yaw." Ocean Engineering 273 (April). https://doi.org/10.1016/j.oceaneng.2023.113961.
39. Yuan, Weixing, Alanna Wall, and Richard Lee. 2018a. "Combined Numerical and Experimental Simulations of Unsteady Ship Airwakes." Computers & Fluids 172:29–53. https://doi.org/https://doi.org/10.1016/j.compfluid.2018.06.006.
40. ———. 2018b. "Combined Numerical and Experimental Simulations of Unsteady Ship Airwakes." Computers and Fluids 172:29–53. https://doi.org/10.1016/j.compfluid.2018.06.006.